Functional characterization of a subtilisin-like serine protease from *Vibrio cholerae*

Received for publication, January 26, 2019, and in revised form, May 7, 2019 Published, Papers in Press, May 10, 2019, DOI 10.1074/jbc.RA119.007745

Matthew Howell[‡§1], Daniel G. Dumitrescu[‡§¶1,2], Lauren R. Blankenship[‡§], Darby Herkert[‡§], and Stavroula K. Hatzios[‡§¶3]

From the Departments of [‡]Molecular, Cellular, and Developmental Biology and [¶]Chemistry, Yale University, New Haven, Connecticut 06511 and the [§]Microbial Sciences Institute, Yale University, West Haven, Connecticut 06516

Edited by Chris Whitfield

***Vibrio cholerae*, the causative agent of the human diarrheal disease cholera, exports numerous enzymes that facilitate its adaptation to both intestinal and aquatic niches. These secreted enzymes can mediate nutrient acquisition, biofilm assembly, and *V. cholerae* interactions with its host. We recently identified a *V. cholerae*-secreted serine protease, IvaP, that is active in *V. cholerae*-infected rabbits and human choleric stool. IvaP alters the activity of several host and pathogen enzymes in the gut and, along with other secreted *V. cholerae* proteases, decreases binding of intelectin, an intestinal carbohydrate-binding protein, to *V. cholerae in vivo*. IvaP bears homology to subtilisin-like enzymes, a large family of serine proteases primarily comprised of secreted endopeptidases. Following secretion, IvaP is cleaved at least three times to yield a truncated enzyme with serine hydrolase activity, yet little is known about the mechanism of extracellular maturation. Here, we show that IvaP maturation requires a series of sequential N- and C-terminal cleavage events congruent with the enzyme's mosaic protein domain structure. Using a catalytically inactive reporter protein, we determined that IvaP can be partially processed in *trans*, but intramolecular proteolysis is most likely required to generate the mature enzyme. Unlike many other subtilisin-like enzymes, the IvaP cleavage pattern is consistent with stepwise processing of the N-terminal propeptide, which could temporarily inhibit, and be cleaved by, the purified enzyme. Furthermore, IvaP was able to cleave purified intelectin, which inhibited intelectin binding to *V. cholerae*. These results suggest that IvaP plays a role in modulating intelectin–*V. cholerae* interactions.**

Vibrio cholerae is a Gram-negative bacterium that thrives in aquatic reservoirs and in the human small intestine, where it can trigger the severe diarrheal disease cholera (1). Infection is caused by the ingestion of food or water contaminated with *V. cholerae*. The bacterium colonizes the intestinal epithelium, where it expresses key virulence genes that induce a massive secretory diarrhea, in which *V. cholerae* is shed from the host (2). Within aquatic ecosystems, *V. cholerae* can subsist on the chitinous surfaces of crustaceans and plankton (3). The ability of *V. cholerae* to persist in aquatic habitats contributes to its rapid dissemination through human populations that lack access to clean water, as recently demonstrated by the explosive epidemics in Haiti and Yemen (4, 5).

The transition of *V. cholerae* from the host intestine to aquatic reservoirs relies in large part on secreted enzymes. Cholera toxin, a paradigmatic AB_5 toxin secreted by *V. cholerae*, is the principal virulence factor responsible for stimulating fluid loss from the gut (2). Hemagglutinin/protease enhances *V. cholerae* detachment from intestinal epithelial cells and, along with other secreted proteases, can contribute to the extracellular processing of cholera toxin (6, 7). Chitin-degrading enzymes promote *V. cholerae* growth in marine and freshwater environments by facilitating bacterial sequestration of nutrients from chitinous surfaces and mediating the formation of biofilms, surface-associated bacterial communities that enhance *V. cholerae* infectivity (3, 8). Enzymes that enable *V. cholerae* to cycle between intestinal and aquatic niches could be targeted to help curb the spread of cholera.

Using a chemical proteomic approach, we recently identified a number of pathogen-secreted serine hydrolases that were active during *V. cholerae* growth in the cecal fluid of *V. cholerae*-infected rabbits and in biofilm cultures (9). One of these enzymes, named IvaP (for *in vivo*–activated protease), was also active in human choleric stool. IvaP was found to alter the activity of other serine hydrolases in the gut, including the host enzymes kallikrein 1 and cholesterin esterase and the pathogen enzymes VCA0812, VolA, VCA0218, and VesB (9). In addition, along with three other secreted *V. cholerae* enzymes (VesA, VesB, and VCA0812), IvaP reduced the abundance and binding of intelectin to the *V. cholerae* cell surface *in vivo* (9). Intelectin is a calcium-dependent, carbohydrate-binding protein produced by mammals, fish, and amphibians that selectively recognizes microbial glycans (10, 11). Intestinal expression of intelectin increases following nematode infection and microbial colonization of germ-free mice (12–14), suggesting that intelectin may play a role in the innate immune response to enteric microbes. Intelectin degradation by IvaP and/or other *V. cholerae* proteases could inhibit intelectin activity during infection, although direct cleavage by these proteases has not been demonstrated. IvaP has also been shown to play an accessory role in

This work was supported by new faculty start-up funds from Yale University (to S. K. H.). The authors declare that they have no conflicts of interest with the contents of this article. The content is solely the responsibility of the authors and does not necessarily represent the official views of the National Institutes of Health.

This article contains Tables S1–S3 and Figs. S1–S8.

[1] Both authors contributed equally to this work.

[2] Supported by National Institutes of Health Chemistry-Biology Interface Predoctoral Training Grant T32GM067543.

[3] To whom correspondence should be addressed. Tel.: 203-737-8121; E-mail: stavroula.hatzios@yale.edu.

biofilm recruitment and dispersal (15, 16), processes that are likely important for *V. cholerae* survival in aquatic reservoirs.

IvaP is homologous to subtilisin-like enzymes (also known as subtilases), which belong to the S8 family of serine peptidases (17). The S8 family includes enzymes from bacteria, archaea, and eukaryotes with diverse substrate specificities and biological activities. Many subtilases contribute to catabolic processes through nonselective protein degradation, whereas others catalyze the selective cleavage of protein precursors, peptide hormones, or growth factors at highly specific sites (18). Subtilases share a conserved catalytic triad in the order of Asp, His, and Ser and normally contain an N-terminal peptidase inhibitor I9 domain, which serves as an intramolecular chaperone and temporary inhibitor of protease activity (17, 19). The I9 domain is a propeptide that is cleaved by the peptidase domain during protein folding, separating the propeptide from the mature enzyme (19). The excised propeptide remains noncovalently bound to the enzyme's active site, forming an autoinhibited complex (18). Subsequent degradation of the propeptide is typically catalyzed by its cognate peptidase or by another active molecule of the protease in *trans* (20).

Like other subtilases, IvaP undergoes extensive post-translational processing (9). Multiple extracellular cleavage events contribute to IvaP maturation, and peptide sequences corresponding to the active enzyme in biofilm culture supernatants and in rabbit cecal fluid suggest that proteolysis occurs at both the N and C terminus (Fig. S1) (9). In addition, IvaP contains a C-terminal bacterial prepeptidase PPC domain that is not typically found in subtilases but facilitates the secretion of other prokaryotic enzymes and is often cleaved extracellularly (17). The mosaic domain structure of IvaP suggests a unique process of proteolytic maturation; however, the molecular mechanism of IvaP processing has not been characterized.

Here, we demonstrate that IvaP maturation requires sequential proteolysis of the enzyme's N and C terminus via intermolecular and intramolecular cleavages. In contrast to classic bacterial subtilisins, cleavage of the IvaP propeptide is consistent with a stepwise mechanism of autoprocessing that results in several intermediates. We show that IvaP is temporarily inhibited by the purified propeptide domain, which is also a substrate for the purified enzyme. In addition, we show that IvaP catalyzes intelectin cleavage *in vitro*. Proteolysis inhibits intelectin binding to *V. cholerae* cells, providing a possible mechanism for how *V. cholerae* subverts this host–pathogen interaction *in vivo*. Taken together, these findings indicate that the extracellular activation of IvaP is regulated by an unconventional mechanism of autoprocessing that could be targeted to inhibit protease activity and potentially alter pathogen interactions with the host.

Results

IvaP undergoes sequential N- and C-terminal processing

We previously demonstrated that autoproteolysis contributes to IvaP processing (9). Mutation of the catalytic Ser-361 to an alanine (*V. cholerae* S361A) caused IvaP^{S361A} to migrate with a molecular mass of ~47 kDa in biofilm culture supernatants; in contrast, IvaP from WT *V. cholerae* migrated with a molecular mass of ~38 kDa, corresponding to the fully processed enzyme. We repeated our analysis of IvaP processing using stationary-phase culture supernatants treated with fluorophosphonate (FP)[4]-TAMRA, a fluorescent activity-based probe for serine hydrolases (21), and detected three major IvaP species (~38, ~44, and ~47 kDa) from WT *V. cholerae* C6706 by in-gel fluorescence and immunoblotting (Fig. 1) (see Table 1 for a list of the *V. cholerae* strains used in this study). In addition, we detected a major ~47-kDa band corresponding to IvaP^{S361A} in stationary-phase culture supernatants from *V. cholerae* S361A; a small amount of the fully truncated protein (~38 kDa) was also detected by Western blotting. These data indicate that Ser-361 contributes to successive autoprocessing of IvaP from ~47 to ~38 kDa in stationary-phase cultures, although some cleavage can occur in the absence of catalytically active IvaP. Furthermore, because the expected molecular mass of the full-length enzyme is ~57 kDa, these findings suggest that IvaP^{S361A} can be cleaved to the ~47-kDa form through a mechanism other than autoproteolysis.

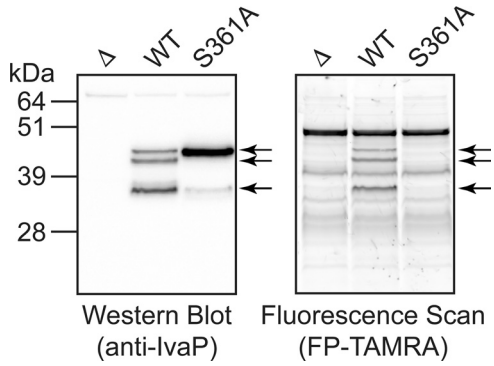

Figure 1. Ser-361 contributes to IvaP autoprocessing in stationary-phase cultures. Shown is Western blotting (*left*) and in-gel fluorescence (*right*) analysis of FP-TAMRA-labeled supernatants from stationary-phase cultures of WT, Δ*ivaP* (Δ), and S361A *V. cholerae* C6706. *Arrows*, IvaP-specific bands. These analyses were repeated three times with consistent results.

We generated epitope-tagged constructs of WT IvaP and IvaP^{S361A} in the arabinose-inducible expression plasmid pBAD33 to analyze the positional processing of the enzyme in stationary-phase culture supernatants. A His_6 tag was cloned immediately downstream of the IvaP signal peptide, along with a C-terminal truncated FLAG (*i.e.* 2× DDDDK) tag. Consistent with our prior analyses of WT *V. cholerae* (Fig. 1), supernatants from Δ*ivaP V. cholerae* expressing the epitope-tagged enzyme (*V. cholerae* WT*) contained three major IvaP* species with serine hydrolase activity (Fig. 2*A*). None of these species retained the His_6 tag, and only the highest-molecular-mass IvaP* precursor (~49 kDa) retained the C-terminal tag. Because we were unable to detect His_6-tagged IvaP*, we reasoned that the enzyme most likely undergoes rapid N-terminal processing under these culture conditions. To inhibit both autoprocessing and potential cleavage by other serine proteases

[4] The abbreviations used are: FP, fluorophosphonate; BisTris, bis(2-hydroxyethyl)iminotris(hydroxymethyl)methane; Bicine, *N*,*N*-bis(2-hydroxyethyl)glycine; CAPS, 3-(cyclohexylamino)propanesulfonic acid; TAMRA, tetramethylrhodamine; SE, succinimidyl ester; PMSF, phenylmethylsulfonyl fluoride; hITLN-1, human intelectin-1; LB, lysogeny broth; gDNA, genomic DNA; nt, nucleotide(s); HK, heat-inactivated IvaP; HRP, horseradish peroxidase; TBS, tris-buffered saline.

Table 1
***V. cholerae* strains used in this study**

Strain	Relevant characteristics[a]	Source/ Reference
WT	WT El Tor O1 clinical isolate of *V. cholerae* C6706 (Sm^R)	Ref. 38
Δ	C6706 Δ*ivaP*	Ref. 9
S361A	C6706 Δ*ivaP*::C6706 $ivaP^{S361A}$	Ref. 9
pBAD	C6706 Δ*ivaP* pBAD33	This study
WT*	C6706 Δ*ivaP* pBAD33*SP-His*$_6$*-ivaP (nt 70–1605)-FLAG*	This study
S361A*	C6706 Δ*ivaP* pBAD33*SP-His*$_6$*-*$ivaP^{S361A}$ *(nt 70–1605)-FLAG*	This study
WT-FLAG	C6706 Δ*ivaP* pBAD33*ivaP-FLAG*	This study
C9Y-FLAG	C6706 Δ*ivaP* pBAD33$ivaP^{C9Y}$*-FLAG*	This study
S361A-His_6	C6706 Δ*ivaP* pBAD33$ivaP^{S361A}$*-*His_6	This study
lacZ::S361A	C6706 *lacZ*::P_{TAC}:$ivaP^{S361A}$*-FLAG*	This study
Δ *lacZ::S361A*	C6706 Δ*ivaP lacZ*::P_{TAC}:$ivaP^{S361A}$*-FLAG*	This study
Haiti	WT El Tor O1 clinical isolate of *V. cholerae*, strain H1 (Sm^R)	Ref. 4
Haiti Δ	Haiti Δ*ivaP*	This study
Y9C	Haiti Δ*ivaP*::$ivaP^{Y9C}$	This study
E7946	WT El Tor O1 clinical isolate (Sm^R)	Ref. 39
E7946 Δ	E7946 Δ*ivaP*	This study
N16961	WT El Tor O1 clinical isolate (Sm^R)	Ref. 40

[a] *ivaP* refers to the *vc0157* gene of *V. cholerae* (NCBI Gene ID 2614886). The FLAG tag used in this study refers to the amino acid sequence DDDDKDDDDK. SP refers to the IvaP signal peptide, amino acids 1–23, encoded by nt 1–69 of the *ivaP* gene.

in solution, we analyzed supernatants from Δ*ivaP V. cholerae* expressing the catalytically inactive enzyme with an N-terminal His_6 and C-terminal FLAG tag (*V. cholerae* S361A*) in the presence of the serine protease inhibitor phenylmethylsulfonyl fluoride (PMSF). PMSF substantially reduced the serine hydrolase activity of S361A* culture supernatants relative to supernatants from cultures expressing empty vector, as indicated by the apparent decrease in FP-TAMRA-labeled proteins (Fig. 2*A*). Western blot analysis revealed a single $IvaP^{S361A*}$ species with intact N- and C-terminal tags that migrated with a molecular mass of ~55 kDa (Fig. 2*A*), consistent with loss of the signal peptide. Together, these findings demonstrate that, following secretion, IvaP* is cleaved at the N terminus to give a ~49-kDa intermediate (~47 kDa for native IvaP) that lacks the N-terminal His_6 tag (Fig. 2*B*). Next, the enzyme is cleaved at the C terminus to ~44 kDa, with a corresponding loss of the C-terminal FLAG tag. The final major processing step most likely occurs at the N terminus. Peptide sequencing data from activity-based proteomic analyses of active IvaP in biofilm culture supernatants (Fig. S1) suggest that IvaP processing results in the loss of ~139 amino acids (~15 kDa) from the IvaP N terminus and ~23 amino acids (~3 kDa) from the IvaP C terminus. These sequencing results are consistent with N-terminal cleavage of the ~44-kDa IvaP intermediate to the fully cleaved ~38-kDa form (9).

IvaP can be partially processed in trans

To investigate the mechanism of IvaP processing, we incubated stationary-phase culture supernatants from S361A* with biofilm culture supernatants from WT *V. cholerae* containing the fully processed form of IvaP. As described under "Experimental procedures," $IvaP^{S361A*}$ expression was induced in the presence of ethanol for 6–7 h to partially inhibit $IvaP^{S361A*}$ proteolysis (our initial attempts to prevent $IvaP^{S361A*}$ proteolysis using PMSF inhibited the serine hydrolase activity of the biofilm culture supernatants used in these assays). The mechanism by which ethanol diminishes $IvaP^{S361A*}$ proteolysis is unclear; bacterial growth attenuation resulting from ethanol treatment may indirectly inhibit the expression and/or activity of other *V. cholerae* protease(s) that cleave $IvaP^{S361A*}$. Western blot analysis revealed that $IvaP^{S361A*}$ is cleaved from ~55 to ~49 kDa in the presence of active IvaP (Fig. 3*A*, *lane 4*). An intermediate precursor of ~52 kDa was also cleaved to ~49 kDa following the addition of WT biofilm supernatants (we occasionally detected this precursor and other minor processing intermediates in our analyses of the IvaP* and $IvaP^{S361A*}$ overexpression constructs). Biofilm culture supernatants from Δ*ivaP V. cholerae* also cleaved $IvaP^{S361A*}$ to ~49 kDa, although the extent of processing was more variable (Fig. 3*A* (*lane 2*) and Fig. S2*A* (*lane 2*)). We did not observe cleavage of $IvaP^{S361A*}$ beyond ~49 kDa using biofilm supernatants from either WT or Δ*ivaP V. cholerae*. Furthermore, WT supernatants were unable to cleave the ~47-kDa precursor produced by *V. cholerae* biofilms expressing chromosomal $IvaP^{S361A}$ (Fig. 3*A*, *lane 7*). Similarly, Western blot analysis of biofilm supernatants from a *V. cholerae* strain expressing chromosomal copies of both WT IvaP and $IvaP^{S361A}$ (*V. cholerae lacZ::S361A*) revealed that the catalytically inactive mutant is not fully cleaved in the presence of endogenous IvaP (Fig. 3*B*, *lane 5*). Together, these data suggest that the initial N-terminal processing event required for IvaP maturation can occur in *trans* and that cleavage of IvaP from ~47 to ~38 kDa occurs via a mechanism of intramolecular proteolysis.

To investigate the mechanism of $IvaP^{S361A*}$ processing by other *V. cholerae* proteases, we grew stationary-phase cultures of *V. cholerae* S361A* and *V. cholerae* WT* in the presence of benzamidine, a reversible inhibitor of trypsin-like enzymes. Unlike S361A* cultures treated with ethanol, cultures grown in the absence of inhibitor produced $IvaP^{S361A*}$ that was partially processed to ~49 kDa by 3 h post-induction (Fig. S2*B*, *lane 2*). Benzamidine decreased processing of $IvaP^{S361A*}$ (Fig. S2*B*, *lane 3*), suggesting that a trypsin-like serine protease can cleave the inactive form of IvaP. In contrast, benzamidine did not inhibit maturation of the catalytically active enzyme in stationary-phase cultures of WT*. These data suggest that although benzamidine-sensitive serine protease(s) can contribute to $IvaP^{S361A*}$ cleavage, autoprocessing may be the dominant mechanism of IvaP maturation.

IvaP exhibits strain-specific processing

We investigated whether IvaP is similarly processed by several pathogenic *V. cholerae* strains. Gel-based fluorescence and Western blot analysis of biofilm culture supernatants from *V. cholerae* C6706, Haiti, E7946, and N16961 revealed a ~38-kDa protein with serine hydrolase activity corresponding to fully processed IvaP (Fig. 4*A*). In addition, three higher-molecular-mass protein species (~44, ~47, and ~55 kDa) were detected in biofilm supernatants from *V. cholerae* Haiti, consistent with the IvaP precursors previously observed in stationary-phase culture supernatants from WT and S361A* *V. cholerae* C6706 (Figs. 1 and 2*A*). One of these proteins (~55 kDa) was also detected in biofilm supernatants from *V. cholerae* N16961. These data demonstrate that IvaP is secreted and active in biofilms produced by several pathogenic *V. cholerae* strains but is

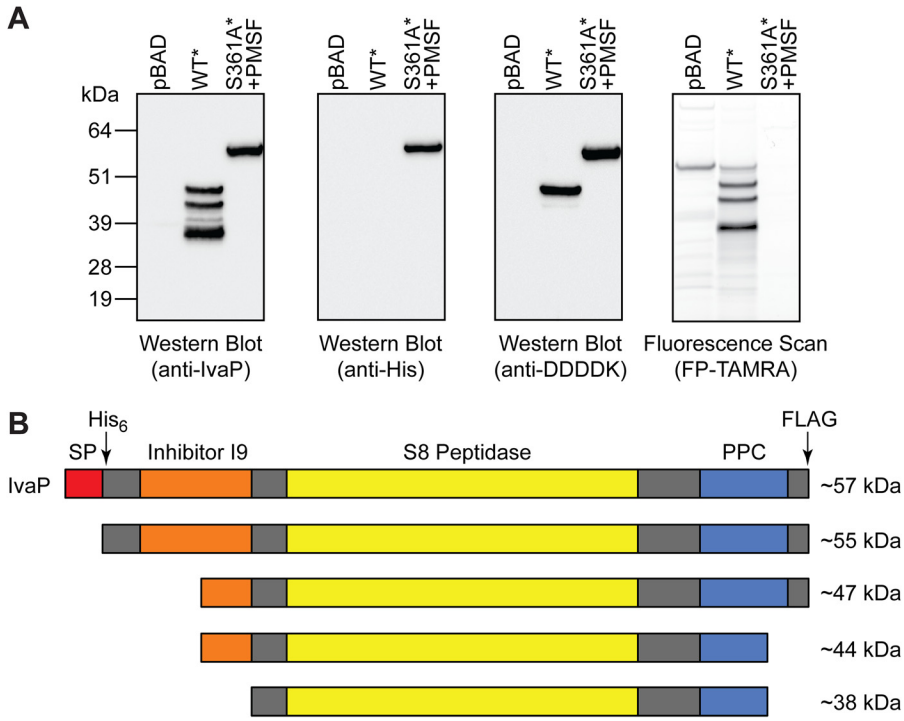

Figure 2. IvaP maturation requires sequential N- and C-terminal processing. *A*, Western blotting (*left*) and in-gel fluorescence (*right*) analysis of FP-TAMRA-labeled supernatants from stationary-phase cultures of Δ*ivaP V. cholerae* C6706 expressing empty vector (pBAD), IvaP* (WT*), or IvaP^{S361A*} (S361A*). Cultures were supplemented with PMSF (S361A*) or vehicle control (pBAD, IvaP*) as described under "Experimental procedures." These analyses were repeated three times with consistent results. *B*, proposed model of the major cleavage events that accompany IvaP maturation. Approximate molecular masses corresponding to native IvaP precursors detected in stationary-phase cultures are shown. The predicted protein domain structure of IvaP was determined using the Simple Modular Architecture Research Tool (version 8.0) (41). *SP*, signal peptide. *PPC*, bacterial prepeptidase PPC domain. The *arrows* indicate positions of His_6 and FLAG tags in IvaP* and IvaP^{S361A*}.

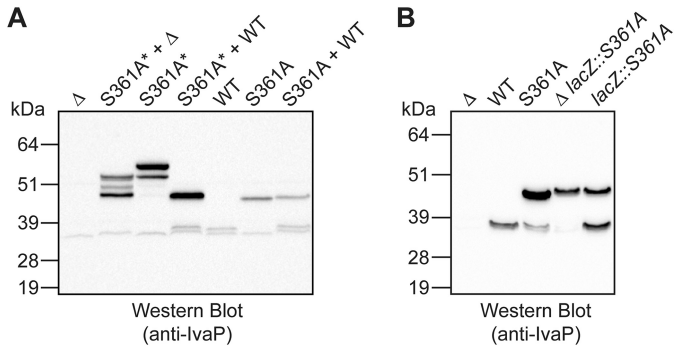

Figure 3. IvaP can be partially processed in *trans*. *A*, Western blot analysis of *V. cholerae* C6706 culture supernatants from Δ*ivaP* (Δ), WT, and S361A biofilms or stationary-phase cultures of S361A*. Cultures of S361A* were supplemented with ethanol to decrease proteolysis of IvaP^{S361A*} as described under "Experimental procedures." Equal protein amounts of WT or Δ and S361A* or S361A supernatants were co-incubated for 1 h at 37 °C prior to analysis. *B*, Western blot analysis of biofilm culture supernatants from Δ, WT, S361A, Δ *lacZ::S361A*, and *lacZ::S361A V. cholerae* C6706. These analyses were repeated three times with consistent results.

incompletely processed by *V. cholerae* Haiti and possibly N16961 under these growth conditions.

C9Y mutation does not affect IvaP processing by V. cholerae Haiti

We considered whether genomic differences might account for the partial processing of IvaP by *V. cholerae* Haiti. Alignment of the *ivaP* sequences from *V. cholerae* C6706 and Haiti revealed a single G-to-A mutation corresponding to the substitution of cysteine with tyrosine at position 9 of the protein encoded by the Haitian *V. cholerae* strain (Fig. S3). This SNP was one of 12 Haiti-specific SNPs detected in a comparative genomic analysis of *V. cholerae* isolates from recent cholera epidemics in Haiti, Asia, and Africa (22). Given that Cys-9 is located within the IvaP signal peptide, we hypothesized that mutation of this residue might inhibit IvaP processing. We mutated Tyr-9 of IvaP to a cysteine in *V. cholerae* Haiti to determine whether this residue influences IvaP maturation. Three IvaP-specific bands were detected in stationary-phase culture supernatants from the WT and mutant (*V. cholerae* Y9C) Haiti strains, consistent with the IvaP species produced by *V. cholerae* C6706 (Fig. S4). In addition, IvaP species from all three strains exhibited similar labeling by FP-TAMRA. However, both WT IvaP from *V. cholerae* Haiti and IvaP^{Y9C} from the mutant strain remained incompletely processed in biofilm culture supernatants (Fig. 4*B*), in contrast to IvaP from *V. cholerae* C6706, which was fully cleaved. These data indicate that the C9Y mutation does not account for the partial post-translational processing of IvaP by *V. cholerae* Haiti.

To determine whether the C9Y mutation interferes with IvaP processing by *V. cholerae* C6706, we expressed *ivaP*^{C9Y} in Δ*ivaP V. cholerae* C6706 (*V. cholerae* C9Y-FLAG) and compared the activity and expression of the encoded protein with that of the WT enzyme expressed by the Δ*ivaP* strain (*V. cholerae* WT-FLAG). Gel-based fluorescence and Western blot analysis of biofilm culture supernatants revealed that both strains produce the fully cleaved enzyme, with no significant accumulation of higher-molecular-mass precursors (Fig. 4*C*).

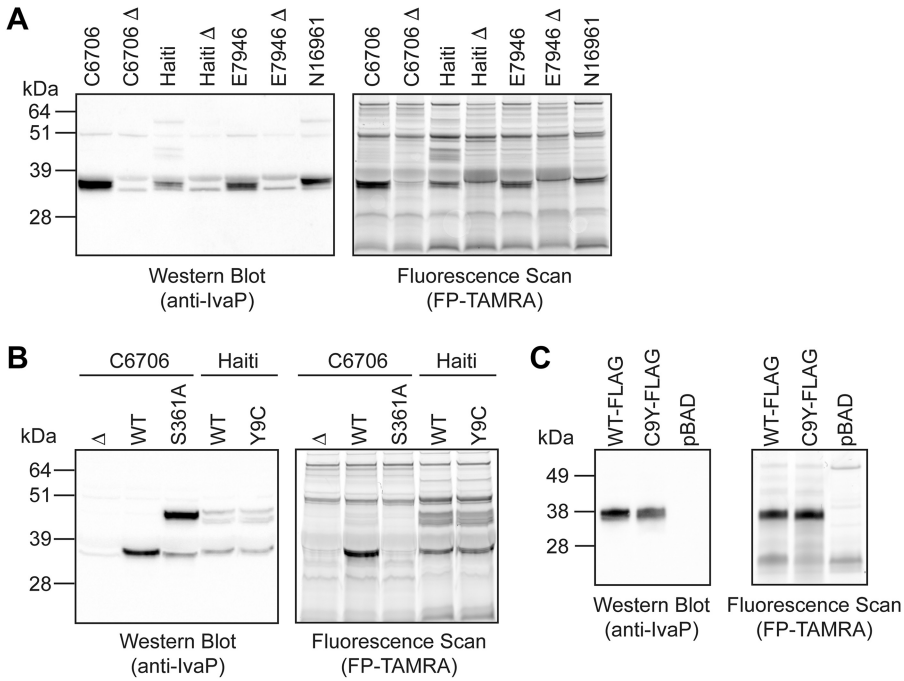

Figure 4. IvaP is incompletely processed by biofilm cultures of *V. cholerae* Haiti. *A*, Western blotting (*left*) and in-gel fluorescence (*right*) analysis of FP-TAMRA-labeled supernatants from biofilm cultures of *V. cholerae* C6706, Haiti, E7946, N16961, and corresponding Δ*ivaP* (Δ) strains. *B*, Western blotting (*left*) and in-gel fluorescence (*right*) analysis of FP-TAMRA-labeled supernatants from biofilm cultures of Δ, WT, and S361A *V. cholerae* C6706 and WT and Y9C *V. cholerae* Haiti. *C*, Western blotting (*left*) and in-gel fluorescence (*right*) analysis of FP-TAMRA-labeled supernatants from biofilm cultures of Δ*ivaP V. cholerae* C6706 expressing IvaP-FLAG (*WT-FLAG*), IvaP^{C9Y}-FLAG (*C9Y-FLAG*), or empty vector (*pBAD*). These analyses were repeated three times with consistent results.

These data demonstrate that the C9Y mutation does not affect IvaP processing, consistent with our findings in *V. cholerae* Haiti. Other factors present in *V. cholerae* Haiti likely contribute to the incomplete processing of IvaP under biofilm growth conditions.

Purification of mature IvaP

Our initial attempts to purify IvaP from *Escherichia coli* using various epitope-tagged expression constructs were unsuccessful. The loss of N- and C-terminal tags during IvaP maturation precluded purification of the mature protease by conventional affinity-based chromatography methods. Furthermore, expression of constructs lacking the I9 domain yielded insoluble protein, consistent with the well-described role of propeptides from the I9 family in protein folding (18, 19). We therefore purified mature IvaP to apparent homogeneity from *V. cholerae* culture supernatants using anion-exchange chromatography (Fig. S5). The purified enzyme exhibited serine hydrolase activity and hydrolyzed the peptide *N*-succinyl-Ala-Ala-Pro-Phe-*p*-nitroanilide, a common substrate of S8 family proteases (Fig. S6) (23). N-terminal sequencing data from Edman degradation analysis of purified IvaP most closely matched the IvaP sequence AAQDNV, which was also the most N-terminal IvaP peptide sequence detected by previous activity-based proteomic analyses of *V. cholerae* biofilm culture supernatants (Fig. S1) (9). These data are consistent with the molecular mass of the fully cleaved enzyme detected in biofilm culture supernatants (~38 kDa; Fig. 3*A*) and with N-terminal processing of the IvaP I9 domain.

pH dependence and chemical inhibition of IvaP activity

We analyzed the effects of pH and of various protease inhibitors on IvaP activity by measuring the relative in-gel fluorescence of the enzyme following incubation with FP-TAMRA. We determined that IvaP is most active at alkaline pH (Fig. 5*A*), similar to other proteases from the S8 family (17). FP-TAMRA labeling was greatest between pH 9 and 10 and was significantly reduced at pH 5. Incubation of IvaP with PMSF also inhibited probe labeling (Fig. 5*B*). In contrast, benzamidine had no effect on IvaP activity, consistent with the observation that benzamidine does not inhibit IvaP* processing in stationary-phase cultures (Fig. S2*B*). Similarly, IvaP activity was unaffected by the metal chelator EDTA, suggesting that IvaP does not require a metal cofactor for catalysis, unlike several prototypical bacterial subtilisins that exhibit calcium-dependent activity (24). A multiple sequence alignment revealed that IvaP lacks a conserved calcium-binding site found in other enzymes from the S8 family (Fig. S7) that may contribute to differences in EDTA sensitivity.

Purified IvaP cleaves mutant precursors in trans

Our initial studies using WT *V. cholerae* biofilm culture supernatants suggested that IvaP can catalyze the N-terminal cleavage of high-molecular-mass IvaP precursors in *trans* (Fig. 3*A*). We treated stationary-phase culture supernatants containing epitope-tagged IvaP^{S361A*} with the purified WT enzyme to determine whether IvaP activity is sufficient for cleavage. Western blot analysis demonstrated that both ~55-kDa and ~52-kDa IvaP^{S361A*} precursors are cleaved to ~49 kDa in the presence of mature IvaP (Fig. 6*A*). IvaP was also able

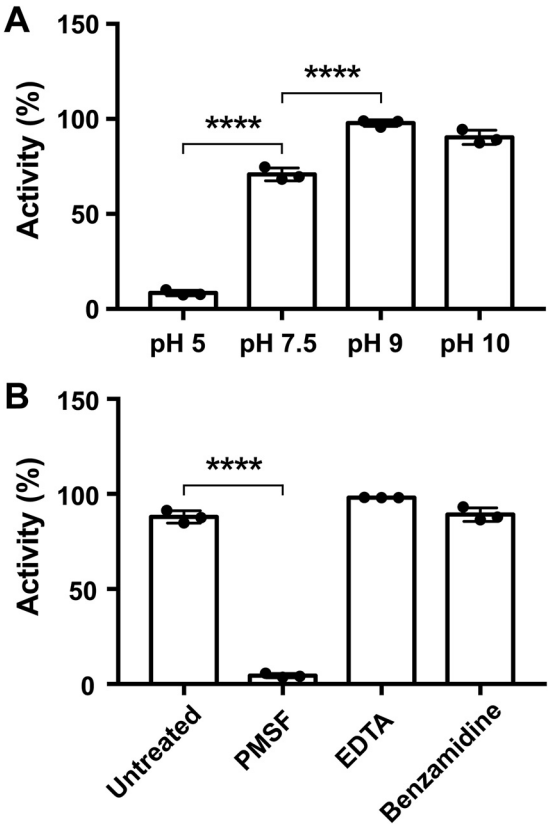

Figure 5. pH dependence and chemical inhibition of IvaP activity. The relative activity of IvaP at different pH (*A*) and in the presence of various protease inhibitors (*B*) was determined by incubating the purified enzyme (500 nM) with FP-TAMRA (2 μM) for 10 min at room temperature and quantifying the in-gel fluorescence intensity of the probe-labeled enzyme by densitometry analysis. Activity measurements represent the mean ± S.D. (*error bars*) of three independent experiments and are reported as a percentage of the maximum observed activity. ****, $p < 0.0001$, one-way analysis of variance with Tukey's (*A*) or Dunnett's (*B*) multiple-comparison test.

to cleave purified mutant precursors in *trans* (Fig. 6*B*), confirming that IvaP^{S361A} is a substrate for the active enzyme.

Inhibitor activity of the IvaP I9 domain

N-terminal processing of IvaP involves cleavage of the enzyme's predicted I9 domain (Fig. S1). In related subtilases, the I9 domain functions as both an intramolecular chaperone and temporary inhibitor that is cleaved during protease maturation (18, 19). To determine whether the I9 domain of IvaP inhibits the mature enzyme, we purified a 111-amino acid region of IvaP (Fig. S8) containing a sequence with homology to previously characterized I9 domains and analyzed the ability of this propeptide to inhibit labeling of purified IvaP by FP-TAMRA. We observed substantially reduced probe labeling of the enzyme in the presence of the I9 domain (Fig. 6*C*), suggesting that the purified propeptide competes with FP-TAMRA for access to the IvaP active site. Similarly, propeptide addition selectively reduced the amount of probe-labeled IvaP in WT *V. cholerae* biofilm culture supernatants (Fig. 6*D*). In both cases, probe labeling of IvaP increased over time, suggesting that the purified I9 domain functions as a temporary inhibitor that is degraded by the enzyme. To confirm this, we evaluated the ability of purified IvaP to cleave the I9 propeptide by SDS-PAGE. Following the addition of purified IvaP, we observed a decrease in the amount of full-length propeptide over time, corresponding with the accumulation of several low-molecular-mass products (Fig. 6*E*). Degradation of the I9 domain depended on IvaP activity; no cleavage was detected in the absence of IvaP or following propeptide incubation with the acid-denatured protease. Together, these data demonstrate that the IvaP propeptide can temporarily inhibit, and be cleaved by, the active enzyme.

IvaP inhibits intelectin binding to V. cholerae

We previously demonstrated that intelectin binds to *V. cholerae in vitro* and in the cecal fluid of *V. cholerae*-infected rabbits (9). In addition, *V. cholerae* lacking IvaP and three other pathogen-secreted proteases was bound by more intelectin *in vivo*, and cecal fluid from rabbits infected with this mutant strain degraded intelectin more slowly *in vitro* than fluid from rabbits infected with WT *V. cholerae* (9). Although these findings suggest that IvaP may contribute to intelectin degradation, direct cleavage of intelectin by IvaP has not been demonstrated.

To determine whether intelectin is a direct substrate for IvaP, we assessed the ability of the purified enzyme to cleave human intelectin-1 (hITLN-1) by SDS-PAGE. hITLN-1, an intelectin isoform produced by the human intestine during cholera, binds to glycans as a disulfide-linked trimer (11, 25, 26). In the absence of IvaP, we detected a major band of ~115 kDa, which corresponds to the molecular mass of purified hITLN-1 in trimeric form (Fig. 7*A*). This species was cleaved to multiple low-molecular-mass products following IvaP treatment. Heat inactivation of IvaP activity inhibited intelectin cleavage. Notably, the major hITLN-1 cleavage product we detected following IvaP treatment migrated with a molecular mass of ~42 kDa, which corresponds to the apparent molecular mass of hITLN-1 in its reduced, monomeric form. Furthermore, incubation of reduced hITLN-1 with IvaP generated a series of cleavage products consistent with those observed following proteolysis of trimeric hITLN-1. These data suggest that IvaP disrupts intelectin oligomers via proteolytic cleavage.

We evaluated whether IvaP-mediated cleavage of hITLN-1 affects its binding to *V. cholerae*. We treated hITLN-1 with WT IvaP, the heat-inactivated enzyme, or a buffer-only (*i.e.* mock-treated) control prior to incubation with *V. cholerae* and analyzed the relative amount of hITLN-1 in unbound, wash, and elution fractions by SDS-PAGE and immunoblotting as described previously (9). We detected a major band corresponding to trimeric intelectin (~115 kDa) in the unbound and elution fractions of cells incubated with either mock-treated hITLN-1 or hITLN-1 treated with heat-inactivated IvaP (Fig. 7*B*). This band was not detected in our analyses of cells incubated with IvaP-treated intelectin; in contrast, a broad, lower-molecular-mass band was detected in the unbound fraction of these cells. Treatment of this fraction with the reducing agent DTT revealed the same low-molecular-mass species produced by IvaP cleavage of intelectin (Fig. 7*C*), indicating that cleaved intelectin can form mixed disulfides that do not bind to *V. cholerae*. In addition, hITLN-1 was not detected in the elution fractions of cells preincubated with EDTA (Fig. 7*D*), consistent with the calcium-dependent binding of intelectin to *V. chol-*

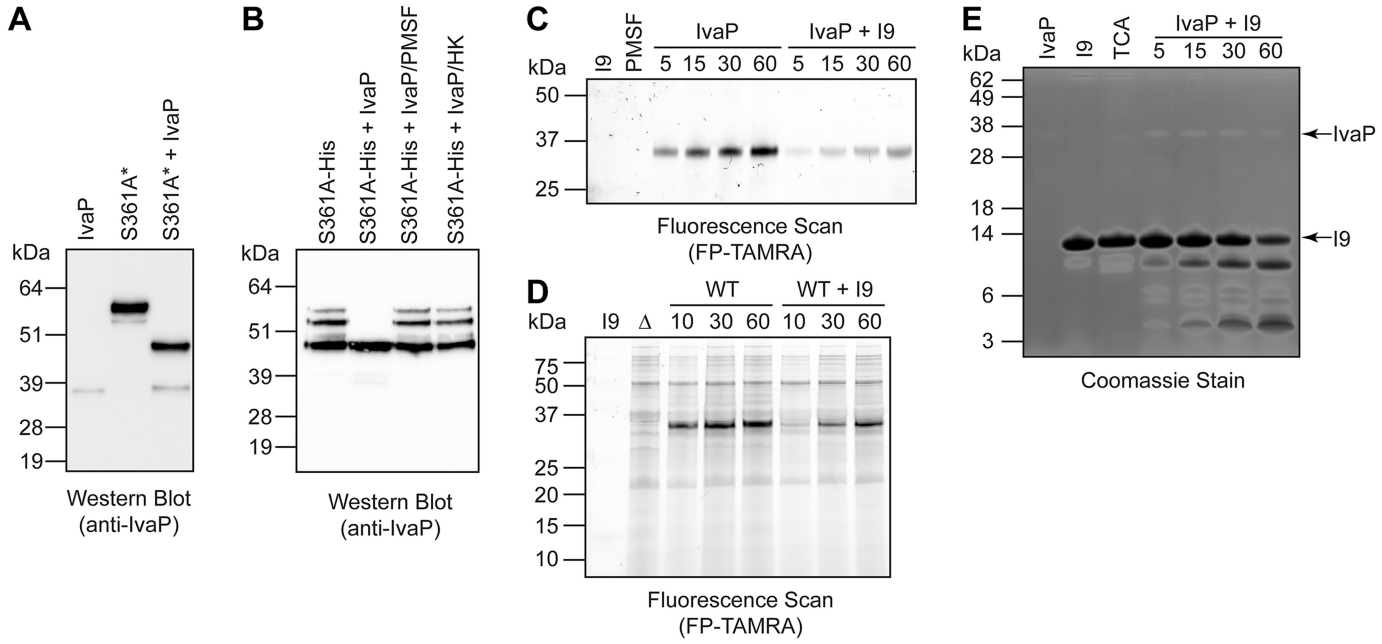

Figure 6. The IvaP I9 domain is a temporary inhibitor and substrate of purified IvaP. Purified IvaP was incubated with stationary-phase culture supernatants from S361A* *V. cholerae* (*A*) or with purified IvaP^{S361A}-His$_6$ precursors (*B*) for 1 h at 37 °C prior to Western blot analysis. Cultures of S361A* were supplemented with ethanol to decrease proteolysis of IvaP^{S361A*} as described under "Experimental procedures." IvaP was pretreated with PMSF or heat-inactivated for 10 min at 95 °C (*HK*) for control experiments. *C*, purified IvaP was incubated with FP-TAMRA in the presence or absence of the purified I9 domain for 5–60 min at room temperature prior to in-gel fluorescence analysis. *I9*, propeptide alone treated with FP-TAMRA for 60 min. *PMSF*, IvaP alone pre-incubated with PMSF prior to treatment with FP-TAMRA for 60 min. As described under "Experimental procedures," the molecular masses of the fluorescent protein standards are approximate. *D*, WT *V. cholerae* C6706 biofilm culture supernatants (WT) were incubated with FP-TAMRA in the presence or absence of the purified I9 domain for 10–60 min at room temperature prior to in-gel fluorescence analysis. *I9*, propeptide alone treated with FP-TAMRA for 60 min. Δ, biofilm culture supernatants from Δ*ivaP V. cholerae* treated with FP-TAMRA for 60 min. As described under "Experimental procedures," the molecular masses of the fluorescent protein standards are approximate. *E*, purified IvaP was incubated with the purified I9 domain for 5–60 min at 37 °C, followed by SDS-PAGE analysis and Coomassie staining. *IvaP*, IvaP alone incubated at 37 °C for 60 min. *I9*, propeptide alone incubated at 37 °C for 60 min. *TCA*, acid-inactivated IvaP incubated with the purified I9 domain for 60 min. These analyses were repeated three times with consistent results.

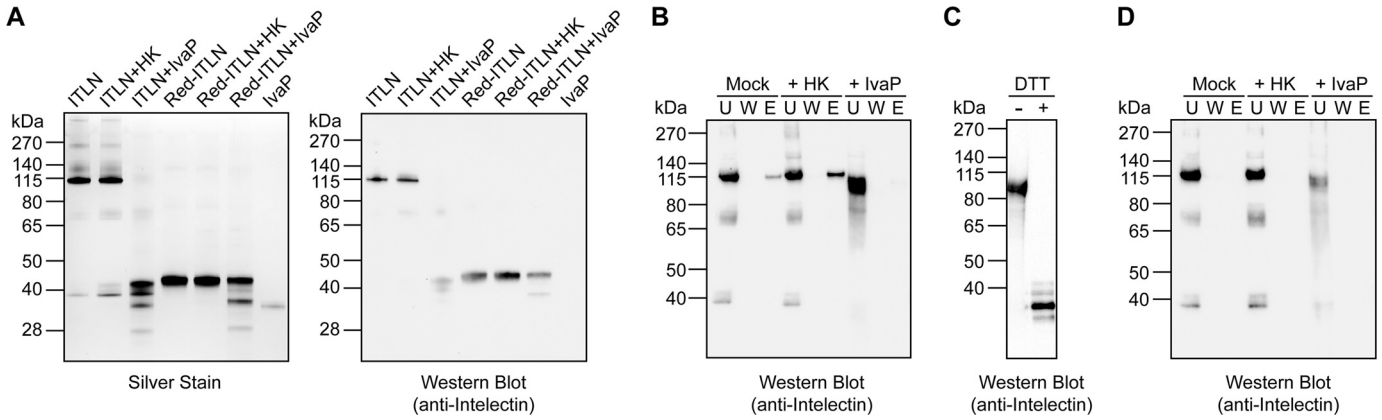

Figure 7. IvaP inhibits hITLN-1 binding to *V. cholerae*. *A*, recombinant hITLN-1 (*ITLN*) was incubated with purified IvaP or heat-inactivated IvaP (HK) for 10 min at room temperature prior to analysis by SDS-PAGE under nonreducing conditions. The same analysis was performed using hITLN-1 treated with reducing agent (*Red-ITLN*) prior to IvaP addition. Proteins were detected by silver staining (*left*) and immunoblotting (*right*). *B*, Western blot analysis of hITLN-1 treated with purified IvaP, HK, or buffer alone (mock) and incubated with *V. cholerae* cells. Unbound (*U*), wash (*W*), and EDTA-eluted (*E*) protein fractions were analyzed under nonreducing conditions. *C*, Western blot analysis of hITLN-1 in the unbound protein fraction following treatment with purified IvaP and incubation with *V. cholerae* cells. Half of the sample was treated with DTT prior to analysis by SDS-PAGE. *D*, Western blot analysis of hITLN-1 treated with purified IvaP, HK, or buffer alone (*Mock*) and incubated with *V. cholerae* cells in the presence of 10 mM EDTA. Unbound (*U*), wash (*W*), and EDTA-eluted (*E*) protein fractions were analyzed under nonreducing conditions. These analyses were repeated two (*C*) or three (*A*, *B*, and *D*) times with consistent results.

erae. Together, these data demonstrate that intelectin binding to *V. cholerae* is inhibited by IvaP activity.

Discussion

In this study, we define the major autoprocessing events that accompany maturation of IvaP, a subtilisin-like serine protease active in *V. cholerae*-infected rabbits and in human choleric stool (9). We establish the order of IvaP cleavage and demonstrate that whereas certain precursors can be cleaved in *trans*, intramolecular processing is most likely required to generate the mature enzyme. Similar to other bacterial subtilases, IvaP is inhibited by its propeptide, which is severed during IvaP maturation and degraded by the fully processed enzyme. However, our data suggest that cleavage of the IvaP N terminus proceeds

via an unconventional, multistep processing mechanism. The first step, which corresponds to IvaP cleavage from ~55 to ~47 kDa via a possible ~52-kDa intermediate (Fig. 2), may reflect partial proteolysis of the I9 domain. This cleavage can occur in *trans*, consistent with previously described examples of propeptide degradation by other subtilases (27, 28), although we cannot exclude the possibility of rapid intramolecular processing by the WT enzyme. The second step occurs following C-terminal cleavage of the enzyme and results in the removal of an additional ~6 kDa from the N terminus, most likely through an intramolecular mechanism of proteolysis (Fig. 2 and Fig. S1). In contrast to other bacterial subtilases (27, 29), we were unable to detect the intact IvaP propeptide during protease maturation, consistent with stepwise processing. The mosaic domain structure of IvaP may influence its maturation process; other proteases with both N- and C-terminal extensions, such as vibriolysin MCP-02, which contains two C-terminal PPC domains, have been shown to undergo stepwise N-terminal processing (30).

How autoproteolysis is initiated remains unclear. Conformational changes induced by the alkaline pH of *V. cholerae* biofilm culture supernatants or the cecal fluid of *V. cholerae*-infected rabbits may play a role. Alternatively, another *V. cholerae* serine protease may facilitate early processing events. Once an initial subset of enzymes is cleaved, activation of the remaining population may occur in *trans*, enabling the amplification of protease activity via propeptide cleavage. The IvaP propeptide appears to be a fairly selective inhibitor of the mature enzyme, based on gel-based analyses of serine hydrolase activity in biofilm culture supernatants (Fig. 6*D*). The propeptide could thus serve as a starting point for the design of more stable inhibitors that could be used to block IvaP activity during infection. Further experimentation is needed to characterize the contributions of specific propeptide sequences to IvaP folding, cleavage, and inhibition.

Unlike many subtilases, IvaP does not appear to require calcium for activity. Bacterial subtilisins typically bind two calcium ions that are essential for protease function and stability (24). One of these ions is coordinated by a well-conserved, high-affinity binding site formed by the side chains and carbonyl oxygen atoms of six amino acids (site 1) (31); none of these residues are conserved in IvaP (Fig. S7), suggesting that site 1 is absent from the enzyme. The absence of this calcium-binding site may explain why IvaP retains serine hydrolase activity in the presence of EDTA. Tk-SP, a subtilase from the archaeon *Thermococcus kodakarensis*, also lacks many of the amino acids found in site 1 and remains active following EDTA treatment (32). Unlike other bacterial subtilisins (*e.g.* subtilisin E, subtilisin Carlsberg), IvaP contains up to seven cysteine residues that may minimize the enzyme's dependence on calcium for structural stability (Fig. S1). IvaP may also contain other calcium-binding sites that promote structural integrity but are dispensable for enzymatic activity.

IvaP is secreted by several pathogenic *V. cholerae* strains but is incompletely processed by *V. cholerae* Haiti, a recent outbreak strain that contains a nonsynonymous SNP in the *ivaP* gene (Fig. S3) (22). The conservation of this SNP among recently sequenced Haitian isolates of *V. cholerae* suggests *ivaP* may be under selective pressure. Although IvaP is not required for *V. cholerae* intestinal colonization in infant rabbits (9), it may play a role in the transition of *V. cholerae* from the host intestine to aquatic reservoirs. Activity-based proteomic analyses of *V. cholerae* biofilm culture supernatants suggest that IvaP enhances the activity of VCA0027 and VCA0700 (9), two chitin-degrading enzymes that are important for bacterial survival in freshwater environments (3). In addition, IvaP shares ~50% amino acid-based sequence identity with peptidases from several marine Gram-negative bacteria, including *Shewanella* and *Pseudoalteromonas* species (33). Strain-specific differences in IvaP processing could be a means of tuning proteolytic activity to different aquatic niches.

Finally, our data suggest that IvaP may directly inhibit intelectin binding to *V. cholerae* in the intestine. Intelectin selectively recognizes nonmammalian sugars and binds to diverse bacterial species, suggesting that it may play a role in intestinal immunity or may alternatively enhance bacterial adhesion to epithelial surfaces (9, 11, 34). IvaP induces disassembly of the hITLN-1 trimer, which likely renders the protein more susceptible to further proteolysis. These findings are in line with our prior observations of enhanced *in vivo* binding of intelectin to *V. cholerae* lacking IvaP and other pathogen-secreted proteases (9). Proteolytic degradation of intelectin could suppress host immunity or facilitate bacterial release from the intestine. Given its ability to recognize a variety of microbial glycans (11), intelectin is likely a substrate for other bacterial proteases. Further characterization of the IvaP–intelectin interaction could reveal strategies for modulating intelectin binding to *V. cholerae* and other microbes.

Experimental procedures

Growth conditions and media

Complete lists of the bacterial strains, plasmids, and primers used in this study are provided in Tables S1–S3. *V. cholerae* and *E. coli* strains were grown at 37 °C in LB medium or on LB agar plates supplemented as needed with 200 μg/ml streptomycin, 50 μg/ml carbenicillin, 50 μg/ml kanamycin, 5 μg/ml chloramphenicol (*V. cholerae*), or 20 μg/ml chloramphenicol (*E. coli*). Stationary-phase cultures (A_{600} ~2–4) were grown with shaking at 250 rpm for 6 h from overnight cultures diluted 1:100 in LB medium. Biofilm cultures were grown in 6-well cell-culture plates without shaking at 37 °C for 48 h from overnight cultures diluted 1:1000 in LB medium. Expression of pBAD33 constructs was induced by supplementing cultures with 0.2% (w/v) L-arabinose at A_{600} ~0.5 for 6–7 h (stationary-phase cultures) or by adding 0.2% (w/v) L-arabinose to the culture medium prior to inoculation (biofilm cultures). Where indicated, cultures of S361A* were supplemented with either 1.25 mM PMSF (Sigma) dissolved in ethanol or an equivalent volume of ethanol alone at the time of induction and every 1.5 h thereafter to prevent or decrease IvaP^{S361A*} proteolysis, respectively. Cultures of WT* and pBAD were supplemented with an equivalent volume of ethanol for comparative analyses with S361A*. Stationary-phase cultures grown in the presence of benzamidine were prepared by supplementing cultures with 0.2% (w/v) L-arabinose and 5 mM benzamidine hydrochloride (pH 8) dis-

solved in water at A_{600} ~0.5 for 3 h. Control samples were prepared by supplementing cultures with an equivalent volume of water at the time of induction.

Strain and plasmid construction

Plasmid construction was performed in *E. coli* DH5α*λpir*, and *E. coli* SM10*λpir* was used for conjugation with *V. cholerae*. Cloned constructs were confirmed by DNA sequencing (for primers, see Table S3) and transformed into *E. coli* and *V. cholerae* strains via electroporation and/or heat shock transformation. Mutant strains of *V. cholerae* were generated using standard allele exchange techniques and derivatives of the suicide plasmids pCVD442 or pTD101, as described previously (35, 36), and were validated by PCR.

V. cholerae Haiti Δ*ivaP* and E7946 Δ*ivaP* were generated using plasmid pCVD442Δ*ivaP* as described previously (9). *V. cholerae* Haiti Δ*ivaP::ivaP*^{Y9C} (Y9C) was generated using plasmid pCVD442*ivaP*^{Y9C} and Haiti Δ*ivaP* as the recipient strain. *V. cholerae* C6706 *lacZ::S361A* and Δ*ivaP lacZ::S361A* were generated using plasmid pTD101*ivaP*^{S361A}*-FLAG* and WT C6706 or C6706 Δ*ivaP* as the recipient strain, respectively. *V. cholerae* strains harboring pBAD33 or its derivatives were generated via electroporation of the specified plasmid into *V. cholerae* C6706 Δ*ivaP*. *E. coli* pET28b*His*$_6$*-I9* was generated via heat-shock transformation of chemically competent *E. coli* OneShot^{TM}BL21(DE3)pLysS cells with pET28b*His*$_6$*-I9*.

Plasmid pCVD442*ivaP*^{Y9C} was constructed by PCR amplification of the *ivaP* gene (*vc0157*; NCBI Gene ID 2614886) with flanking regions from *V. cholerae* C6706 gDNA using primers SKH-147 and SKH-150. The resulting PCR product was digested with XbaI and ligated into pCVD442 plasmid digested with the same enzyme.

Plasmid pET28b*ivaP-His*$_6$ was constructed by PCR amplification of the *ivaP* gene from *V. cholerae* C6706 gDNA using primers SKH-196 and SKH-197. The resulting PCR product was digested with NcoI and XhoI and ligated into pET28b plasmid digested with the same enzymes. The encoded Ser-361 was mutated to alanine by QuikChange mutagenesis (Agilent) using primers SKH-170 and SKH-171 to give plasmid pET28b*ivaP*^{S361A}*-His*$_6$.

Plasmid pET28b*His*$_6$*-ivaP(nt 70–1605)-His*$_6$ was constructed by PCR amplification of nt 70–1605 of the *ivaP* gene using plasmid pCVD442*ivaP*^{Y9C} as template and primers SKH-198 and SKH-199. The resulting PCR product was digested with NdeI and XhoI and ligated into pET28b plasmid digested with the same enzymes.

Plasmid pET28b*His*$_6$*-I9* was constructed by PCR amplification of nt 70–402 of the *ivaP* gene using plasmid pET28b*ivaP-His*$_6$ as template and primers DD-3 and DD-4. The resulting PCR product was cloned by Gibson assembly (37) into pET28b digested with NcoI.

Plasmid pBAD33*ivaP-FLAG* was constructed by PCR amplification of the *ivaP* gene from *V. cholerae* C6706 gDNA using primers SKH-231 and SKH-233. The resulting PCR product was cloned by Gibson assembly into pBAD33 digested with Eco53kI. The encoded Cys-9 was mutated to tyrosine by QuikChange mutagenesis using primers DMH-1 and DMH-2 to give plasmid pBAD33*ivaP*^{C9Y}*-FLAG*.

Plasmids pBAD33*ivaP*^{S361A}*-FLAG* and pBAD33*ivaP*^{S361A}*-His*$_6$ were constructed by PCR amplification of the *ivaP*^{S361A} gene using plasmid pET28b*ivaP*^{S361A}*-His*$_6$ as template and primers SKH-231 and SKH-233 or SKH-231 and SKH-232, respectively. The resulting PCR products were cloned by Gibson assembly into pBAD33 digested with Eco53kI.

pBAD33*SP-His*$_6$*-ivaP-FLAG* was constructed by PCR amplification of nt 70–1605 of the *ivaP* gene using plasmid pET28b*His*$_6$*-ivaP(nt 70–1605)-His*$_6$ as template and primers SKH-233 and SKH-236. A 5′ extension encoding nt 1–69 of the *ivaP* gene was annealed to the resulting PCR product using primers SKH-239 and SKH-240. The final PCR product was cloned by Gibson assembly into pBAD33 digested with Eco53kI. The encoded Ser-361 was mutated to alanine by QuikChange mutagenesis using primers SKH-170 and SKH-171 to give plasmid pBAD33*SP-His*$_6$*-ivaP*^{S361A}*-FLAG*.

Plasmid pTD101*ivaP*^{S361A}*-FLAG* was constructed by PCR amplification of the *ivaP*^{S361A} gene using plasmid pBAD33*ivaP*^{S361A}*-FLAG* as template and primers SKH-246 and SKH-247. The resulting PCR product was cloned by Gibson Assembly into SmaI-digested pTD101, a *lacZ* integration plasmid with $lacI_q$, P_{TAC}, and a multiple cloning site (kind gift of Tobias Dörr, Cornell University) (36).

Sample preparation for gel-based fluorescence and Western blotting analyses

Stationary-phase cultures were normalized by A_{600} prior to centrifugation (3200 × *g*, 4 °C, 20 min). Supernatants from stationary-phase cultures were vacuum-filtered using 0.22-μm PVDF filters (EMD Millipore) and concentrated by centrifugation (3200 × *g*, 4 °C, 30–60 min) using Amicon Ultra-15 centrifugal filter units with an Ultracel-10 membrane (EMD Millipore). Biofilm cultures were centrifuged (3200 × *g*, 4 °C, 20 min) to isolate culture supernatants, which were subsequently syringe-filtered using 0.22-μm PVDF filters and concentrated by centrifugation (3200 × *g*, 4 °C, 30–60 min) using Amicon Ultra-4 centrifugal filter units with an Ultracel-10 membrane. The Pierce Coomassie Plus assay kit (Thermo Fisher Scientific) was used to quantify protein concentration. Concentrated cell-free supernatants from stationary-phase and biofilm cultures were normalized by total protein concentration (0.25–1 mg/ml) prior to comparative gel-based analyses.

Gel-based fluorescence assays

Samples were reacted with 2 μM FP-TAMRA (ActivX TAMRA-FP serine hydrolase probe; Thermo Fisher Scientific) for 1 h at room temperature except where indicated and were protected from light. Reactions were quenched with 4× NuPAGE LDS sample buffer (Thermo Fisher Scientific) and 1–10 mM DTT for 5–10 min at 95 °C. Samples were resolved by SDS-PAGE using 4–12% or 12% BisTris NuPAGE precast gels with MES or MOPS running buffer (Thermo Fisher Scientific) alongside the SeeBlue prestained protein standard (Thermo Fisher Scientific) and/or a fluorescent ladder generated by reacting Precision Plus Protein unstained standards (Bio-Rad) with 6-carboxytetramethylrhodamine succinimidyl ester (6-TAMRA, SE; AnaSpec). Because the exact increase in molecular mass introduced by the conjugation of 6-TAMRA, SE with

each protein standard is unknown, the molecular masses of the fluorescent ladder are approximate. In-gel fluorescence was detected using a Typhoon FLA 9000 scanner (GE Healthcare) with excitation at 532 nm. Total protein was detected using SimplyBlue SafeStain (also known as Coomassie stain; Thermo Fisher Scientific).

Western blotting analyses

Protein samples were resolved by SDS-PAGE using 4–12% or 12% BisTris NuPAGE precast gels with MES or MOPS running buffer alongside the SeeBlue prestained protein standard or Spectra Multicolor high-range protein ladder (Thermo Fisher Scientific). Proteins were transferred to nitrocellulose membranes following SDS-PAGE using an iBlot 2 Dry Blotting System (Thermo Fisher Scientific). Membranes were blocked with 3% (w/v) dry milk in TBST prior to incubation with a mouse polyclonal anti-IvaP antibody (GenScript; 1:1000–1:2000 dilution) (9), a rabbit polyclonal anti-DDDDK antibody (Abcam ab1162; 1:5,000 dilution), a sheep polyclonal anti-human intelectin-1 antibody (R&D Systems AF4254; 1:2,000 dilution), or one of two mouse monoclonal anti-His antibodies (GenScript A00186 (15 μl per 10 ml of TBST) and Invitrogen MA1–21315 (1:1000 dilution)). Peroxidase-conjugated secondary antibodies (goat anti-rabbit IgG-HRP, Sigma A4914, 1:5000 dilution; goat anti-mouse IgG-HRP, Promega W4021, 1:5000 dilution; and rabbit anti-sheep IgG-HRP, Southern Biotech 6150-05, 1:5000 dilution) and SuperSignal West Pico PLUS chemiluminescent substrate (Thermo Fisher Scientific) were used to detect immunostained proteins with a ChemiDoc Gel Imaging System (Bio-Rad).

Purification of IvaP

Single colonies of C6706 Δ*ivaP* pBAD*ivaP-FLAG* were used to inoculate 20-ml overnight cultures of LB medium containing 5 μg/ml chloramphenicol. Overnight cultures were diluted 1:100 in 1 liter of LB medium containing 5 μg/ml chloramphenicol and grown to A_{600} ~0.6. Expression was induced with 0.2% (w/v) L-arabinose for 4 h at 37 °C. Cells were cleared by centrifugation (20,000 × *g*, 4 °C, 30 min), and the vacuum-filtered supernatant (0.22-μm filter) was subjected to ammonium sulfate precipitation at 60% saturation. The precipitate was harvested by centrifugation (10,800 × *g*, 4 °C, 40 min), resuspended in ~5 ml of Buffer A (50 mM Tris buffer, 1 mM DTT, pH 7.4), and dialyzed against Buffer A. The sample was cleared by centrifugation (3200 × *g*, 4 °C, 20 min), vacuum-filtered (0.22-μm filter), and loaded onto a Mono Q 5/50 GL anion-exchange chromatography column (GE Healthcare) equilibrated with Buffer A using an ÄKTA pure chromatography system (GE Healthcare). The sample was washed with 10 column volumes of Buffer A and eluted using a gradient of 0–75% Buffer B (50 mM Tris buffer, 1 M NaCl, 1 mM DTT, pH 7.4) over 20 column volumes at a constant temperature of 4 °C. Elution fractions (0.5 ml) were resolved by SDS-PAGE, followed by Coomassie staining and Western blot analysis using an anti-IvaP antibody. Fractions containing the purified, fully cleaved form of IvaP (~38 kDa) were flash-frozen and stored at −80 °C. Protein concentration was determined by UV absorbance at 280 nm using a calculated extinction coefficient of 38,390 M^{-1} cm^{-1}, which corresponds to the predicted amino acid sequence of mature IvaP (Fig. S1). The average yield of purified IvaP was ~0.5 mg/liter of cell culture.

Purification of the IvaP I9 domain

Single colonies of *E. coli* OneShot™BL21(DE3)pLysS containing pET28b*His$_6$-I9* were used to inoculate 20-ml overnight cultures of LB medium supplemented with 50 μg/ml kanamycin. Overnight cultures were diluted 1:100 in 1 liter of LB medium containing 50 μg/ml kanamycin and grown to A_{600} ~0.5. Expression was induced with 0.75 mM isopropyl β-D-1-thiogalactopyranoside for 5 h at 37 °C. Cells were harvested by centrifugation (20,000 × *g*, 4 °C, 30 min) and resuspended in ice-cold Buffer C (20 mM Tris buffer, 500 mM NaCl, 30 mM imidazole, 1 mM DTT, pH 7.4, 6 ml/g of cells) supplemented with 1 mg/ml lysozyme (Sigma), 5 μg/ml DNase (VWR), and one complete EDTA-free protease inhibitor tablet (Sigma). Cells were lysed using a handheld tissue homogenizer followed by sonication (QSonica Q500 Sonicator). The lysate was cleared by centrifugation (13,800 × *g*, 4 °C, 20 min), vacuum-filtered (0.22-μm filter), and loaded onto a 1-ml HisTrap FF column (GE Healthcare) equilibrated with Buffer C using an ÄKTA pure chromatography system. The sample was washed with 10 column volumes of Buffer C and eluted using a gradient of 0–100% Buffer D (20 mM Tris buffer, 500 mM NaCl, 500 mM imidazole, 1 mM DTT, pH 7.4) over 20 column volumes at a constant temperature of 4 °C. Elution fractions (0.5 ml) were analyzed by SDS-PAGE and Coomassie staining. Fractions containing the purified I9 domain were pooled and dialyzed against Buffer E (20 mM Tris buffer, 150 mM NaCl, 1 mM DTT, pH 7.4) and then flash-frozen and stored at −80 °C. Protein concentration was determined using the Pierce Coomassie Plus assay kit. The yield of purified I9 domain was ~18 mg/liter of cell culture.

Purification of IvaP^{S361A} precursors

Single colonies of C6706 Δ*ivaP* pBAD*ivaP^{S361A}-His$_6$* were used to inoculate 20-ml overnight cultures of LB medium containing 5 μg/ml chloramphenicol. Overnight cultures were diluted 1:100 in 1 liter of LB medium containing 5 μg/ml chloramphenicol and grown to A_{600} ~0.6. Expression was induced with 0.2% (w/v) L-arabinose for 6 h at 37 °C. Cultures were supplemented with 1 mM PMSF at the time of induction and every 1.5 h thereafter to inhibit proteolysis. Cells were cleared by centrifugation (20,000 × *g*, 4 °C, 30 min), and the vacuum-filtered supernatant (0.22-μm filter) was subjected to ammonium sulfate precipitation at 60% saturation. The precipitate was harvested by centrifugation (10,800 × *g*, 4 °C, 40 min), resuspended in ~6 ml of Buffer C, and dialyzed against Buffer C. The sample was cleared by centrifugation (3200 × *g*, 4 °C, 20 min), vacuum-filtered (0.22-μm filter), and loaded onto a 1-ml HisTrap FF column equilibrated with Buffer C using an ÄKTA pure chromatography system. The sample was washed with 10 column volumes of Buffer C and eluted using a gradient of 0–100% Buffer D over 20 column volumes at a constant temperature of 4 °C. Elution fractions (0.5 ml) were resolved by SDS-PAGE, followed by Coomassie staining and Western blot analysis using an anti-IvaP antibody. Fractions containing purified IvaP^{S361A} precursors were pooled and dialyzed against Buffer F

(20 mM Tris buffer, 150 mM NaCl, pH 7.4), concentrated using Amicon Ultra-15 centrifugal filter units with an Ultracel-10 membrane, and then aliquoted and stored at −80 °C. Protein concentration was determined using the Pierce Coomassie Plus assay kit. The yield of purified IvaP^{S361A} precursors was ~0.1 mg/liter of cell culture.

Edman degradation analysis

Purified IvaP was resolved by SDS-PAGE using a 10% BisTris NuPAGE precast gel and transferred to a PVDF membrane. The membrane was stained with Ponceau S (Sigma), and the relevant band was excised for N-terminal sequencing by Alphalyse (Palo Alto, CA).

Inhibitor and pH assays

For inhibitor assays, reaction mixtures contained 500 nM purified IvaP and 1 mM PMSF, 5 mM EDTA (Fisher), 5 mM benzamidine hydrochloride (Sigma), or no inhibitor in 50 mM HEPES buffer, pH 7.5. For pH assays, reaction mixtures contained 500 nM purified IvaP in 50 mM citrate buffer, pH 5, HEPES buffer, pH 7.5, Bicine buffer, pH 9, or CAPS buffer, pH 10. All samples were preincubated for 10 min at room temperature prior to the addition of 2 μM FP-TAMRA for 10 min at room temperature, protected from light. Reaction mixtures were prepared in triplicate and resolved by SDS-PAGE on a single gel with all other samples from a given assay. In-gel fluorescence was quantified by densitometry analysis using ImageJ (version 1.51). To determine the relative activity of IvaP under different reaction conditions, background-subtracted integrated density measurements from triplicate samples across three independent experiments were averaged and reported as a percentage of the maximum value in each data set. Statistical analyses were performed using GraphPad Prism (version 7.0) using a one-way analysis of variance with Tukey's or Dunnett's multiple-comparison test.

Kinetic analysis of N-succinyl-Ala-Ala-Pro-Phe-p-nitroanilide hydrolysis

Kinetic parameters for cleavage of the colorimetric peptide substrate N-succinyl-Ala-Ala-Pro-Phe-*p*-nitroanilide (Cayman) by IvaP and subtilisin A (Sigma, P5380) were determined under steady-state conditions. Reaction mixtures containing 10 nM enzyme, 100 mM Tris-HCl buffer, pH 8, and 0.1–6 mM substrate were prepared in triplicate. Product formation was measured following a 2-min incubation at room temperature by recording the increase in absorbance at 410 nm with a SpectraMax i3X plate reader (Molecular Devices) (product formation was linear under these conditions). Control reactions containing 1 mM substrate in the absence of enzyme were used to account for background hydrolysis. Background-subtracted absorbance measurements were normalized to a path length of 1 cm and converted to product concentrations using an extinction coefficient of 8800 M^{-1} cm^{-1} for *p*-nitroaniline. Michaelis–Menten kinetic parameters using data from three independent experiments were calculated using GraphPad Prism (version 7.0).

IvaP cleavage of IvaP^{S361A} precursors

Supernatants from WT or Δ*ivaP V. cholerae* C6706 biofilms and stationary-phase S361A* cultures or S361A biofilms were diluted to the same total protein concentration (~0.2 mg/ml) in PBS and incubated alone or in a 1:1 ratio by volume for 1 h at 37 °C. Purified IvaP (84 nM) was incubated with stationary-phase S361A* culture supernatants (~0.2 mg/ml) or purified IvaP^{S361A} precursors (~25 μg/ml) in a 100-μl volume for 1 h at 37 °C. Control reactions were prepared using heat-inactivated IvaP (incubated for 10 min at 95 °C) or IvaP pretreated for 15 min at room temperature with 1 mM PMSF. Samples were treated with 4× NuPAGE LDS sample buffer containing DTT for 10 min at 95 °C prior to SDS-PAGE and Western blot analysis.

Inhibition of IvaP activity by the IvaP I9 domain

Purified IvaP (100 nM) was incubated with 2 μM FP-TAMRA in the presence of the purified IvaP I9 domain (50 μM) or an equivalent volume of water for 1 h at 37 °C, protected from light. Reaction aliquots were removed after 5, 15, 30, and 60 min and quenched with 4× NuPAGE LDS sample buffer and 1 mM DTT for 5 min at 95 °C. Control reactions containing the I9 domain alone or IvaP pretreated for 15 min with 1 mM PMSF were quenched after 60 min. Samples were resolved by SDS-PAGE prior to in-gel fluorescence analysis.

Biofilm culture supernatants (0.5 mg/ml total protein) were incubated with 2 μM FP-TAMRA in the presence of the purified IvaP I9 domain (0.5 mg/ml) or an equivalent volume of water for 1 h at room temperature, protected from light. Reaction aliquots were removed after 10, 30, and 60 min and quenched with 4× NuPAGE LDS sample buffer and 1 mM DTT for 5 min at 95 °C. Control reactions containing the I9 domain alone or biofilm culture supernatants from Δ*ivaP V. cholerae* were quenched after 60 min. Samples were resolved by SDS-PAGE prior to in-gel fluorescence analysis.

IvaP cleavage of the IvaP I9 domain

Purified IvaP (500 nM) was incubated with the IvaP I9 domain (50 μM) for 1 h at 37 °C. Reaction aliquots were removed after 5, 15, 30, and 60 min and quenched with 4× NuPAGE LDS sample buffer and 1 mM DTT for 5 min at 95 °C. Control reactions containing the I9 domain alone, IvaP alone, or IvaP pretreated for 15 min with 2.5% (v/v) TCA were quenched after 60 min. Samples were resolved by SDS-PAGE and visualized by Coomassie staining.

Intelectin cleavage and binding assays

Purified hITLN-1 (0.5 μg; Sigma, SRP8047) was treated with 250–500 nM IvaP, heat-inactivated IvaP (HK; incubated for 30 min at 95 °C), or an equivalent volume of PBS for 5 min at room temperature in PBS. Reactions were quenched with 4× NuPAGE LDS sample buffer in the absence of reducing agent for 5 min at 95 °C prior to analysis by SDS-PAGE and silver staining or immunoblotting. Similar reactions were performed using hITLN-1 pretreated with 4 mM DTT for 10 min at room temperature. For binding assays, hITLN-1 (1 μg) was treated with 250 nM IvaP, HK, or an equivalent volume of PBS for 10

min at room temperature in PBS. Half of each reaction mixture (10 μl) was combined with 20 μl of HEPES-buffered saline containing 2 mM $CaCl_2$ (HSC) and incubated with mid-exponential phase *V. cholerae* C6706 as described previously (9). Samples were washed once with HSC, and bound hITLN-1 was eluted in a TBS solution containing 10 mM EDTA. An identical sample set was prepared by combining the other half of each reaction mixture with HSC supplemented with 10 mM EDTA. Unbound input, wash, and elution fractions were treated with 4× NuPAGE LDS sample buffer in the absence of reducing agent for 5 min at 95 °C prior to SDS-PAGE and Western blot analysis. A portion of the unbound input fraction from *V. cholerae* cells incubated with IvaP-treated hITLN-1 in HSC was separately treated with 5 mM DTT prior to SDS-PAGE analysis.

Author contributions—M. H., D. G. D., and S. K. H. conceptualization; M. H., D. G. D., and S. K. H. data curation; M. H., D. G. D., and S. K. H. formal analysis; M. H., D. G. D., L. R. B., D. H., and S. K. H. investigation; M. H., D. G. D., and S. K. H. methodology; M. H., D. G. D., and S. K. H. writing-original draft; M. H., D. G. D., L. R. B., D. H., and S. K. H. writing-review and editing; S. K. H. supervision; S. K. H. funding acquisition; S. K. H. project administration.

Acknowledgments—We thank Tobias Dörr (Cornell University) and Ankur Dalia (Indiana University) for bacterial strains and reagents. We are grateful to Tobias Dörr (Cornell University) and Sören Abel (University of Tromsø) for feedback on the manuscript.

References

1. Nelson, E. J., Harris, J. B., Morris, J. G., Jr., Calderwood, S. B., and Camilli, A. (2009) Cholera transmission: the host, pathogen and bacteriophage dynamic. *Nat. Rev. Microbiol.* **7,** 693–702 CrossRef Medline
2. Ritchie, J. M., and Waldor, M. K. (2009) *Vibrio cholerae* interactions with the gastrointestinal tract: lessons from animal studies. *Curr. Top. Microbiol. Immunol.* **337,** 37–59 CrossRef Medline
3. Hayes, C. A., Dalia, T. N., and Dalia, A. B. (2017) Systematic genetic dissection of chitin degradation and uptake in *Vibrio cholerae*. *Environ. Microbiol.* **19,** 4154–4163 CrossRef Medline
4. Chin, C. S., Sorenson, J., Harris, J. B., Robins, W. P., Charles, R. C., Jean-Charles, R. R., Bullard, J., Webster, D. R., Kasarskis, A., Peluso, P., Paxinos, E. E., Yamaichi, Y., Calderwood, S. B., Mekalanos, J. J., Schadt, E. E., and Waldor, M. K. (2011) The origin of the Haitian cholera outbreak strain. *N. Engl. J. Med.* **364,** 33–42 CrossRef Medline
5. Weill, F. X., Domman, D., Njamkepo, E., Almesbahi, A. A., Naji, M., Nasher, S. S., Rakesh, A., Assiri, A. M., Sharma, N. C., Kariuki, S., Pourshafie, M. R., Rauzier, J., Abubakar, A., Carter, J. Y., Wamala, J. F., *et al.* (2019) Genomic insights into the 2016–2017 cholera epidemic in Yemen. *Nature* **565,** 230–233 CrossRef Medline
6. Nielsen, A. T., Dolganov, N. A., Otto, G., Miller, M. C., Wu, C. Y., and Schoolnik, G. K. (2006) RpoS controls the *Vibrio cholerae* mucosal escape response. *PLoS Pathog.* **2,** e109 CrossRef Medline
7. Sikora, A. E., Zielke, R. A., Lawrence, D. A., Andrews, P. C., and Sandkvist, M. (2011) Proteomic analysis of the *Vibrio cholerae* type II secretome reveals new proteins, including three related serine proteases. *J. Biol. Chem.* **286,** 16555–16566 CrossRef Medline
8. Tamayo, R., Patimalla, B., and Camilli, A. (2010) Growth in a biofilm induces a hyperinfectious phenotype in *Vibrio cholerae*. *Infect. Immun.* **78,** 3560–3569 CrossRef Medline
9. Hatzios, S. K., Abel, S., Martell, J., Hubbard, T., Sasabe, J., Munera, D., Clark, L., Bachovchin, D. A., Qadri, F., Ryan, E. T., Davis, B. M., Weerapana, E., and Waldor, M. K. (2016) Chemoproteomic profiling of host and pathogen enzymes active in cholera. *Nat. Chem. Biol.* **12,** 268–274 CrossRef Medline
10. Lu, Z. H., di Domenico, A., Wright, S. H., Knight, P. A., Whitelaw, C. B., and Pemberton, A. D. (2011) Strain-specific copy number variation in the intelectin locus on the 129 mouse chromosome 1. *BMC Genomics* **12,** 110 CrossRef Medline
11. Wesener, D. A., Wangkanont, K., McBride, R., Song, X., Kraft, M. B., Hodges, H. L., Zarling, L. C., Splain, R. A., Smith, D. F., Cummings, R. D., Paulson, J. C., Forest, K. T., and Kiessling, L. L. (2015) Recognition of microbial glycans by human intelectin-1. *Nat. Struct. Mol. Biol* **22,** 603–610 CrossRef Medline
12. Cash, H. L., Whitham, C. V., Behrendt, C. L., and Hooper, L. V. (2006) Symbiotic bacteria direct expression of an intestinal bactericidal lectin. *Science* **313,** 1126–1130 CrossRef Medline
13. Pemberton, A. D., Knight, P. A., Gamble, J., Colledge, W. H., Lee, J. K., Pierce, M., and Miller, H. R. (2004) Innate BALB/c enteric epithelial responses to *Trichinella spiralis*: inducible expression of a novel goblet cell lectin, intelectin-2, and its natural deletion in C57BL/10 mice. *J. Immunol.* **173,** 1894–1901 CrossRef Medline
14. Voehringer, D., Stanley, S. A., Cox, J. S., Completo, G. C., Lowary, T. L., and Locksley, R. M. (2007) *Nippostrongylus brasiliensis*: identification of intelectin-1 and -2 as Stat6-dependent genes expressed in lung and intestine during infection. *Exp. Parasitol.* **116,** 458–466 CrossRef Medline
15. Smith, D. R., Maestre-Reyna, M., Lee, G., Gerard, H., Wang, A. H., and Watnick, P. I. (2015) *In situ* proteolysis of the *Vibrio cholerae* matrix protein RbmA promotes biofilm recruitment. *Proc. Natl. Acad. Sci. U.S.A.* **112,** 10491–10496 CrossRef Medline
16. Yan, J., Nadell, C. D., and Bassler, B. L. (2017) Environmental fluctuation governs selection for plasticity in biofilm production. *ISME J.* **11,** 1569–1577 CrossRef Medline
17. Rawlings, N. D., and Barrett, A. J. (2013) Chapter 559–Introduction: Serine peptidases and their clans, in *Handbook of Proteolytic Enzymes*, 3rd Ed. (Rawlings, N.D., and Salvesen, G., eds) pp. 2491–2523, Academic Press, London
18. Shinde, U., and Thomas, G. (2011) Insights from bacterial subtilases into the mechanisms of intramolecular chaperone-mediated activation of furin. *Methods Mol. Biol.* **768,** 59–106 CrossRef Medline
19. Hohl, M., Stintzi, A., and Schaller, A. (2017) A novel subtilase inhibitor in plants shows structural and functional similarities to protease propeptides. *J. Biol. Chem.* **292,** 6389–6401 CrossRef Medline
20. Yabuta, Y., Takagi, H., Inouye, M., and Shinde, U. (2001) Folding pathway mediated by an intramolecular chaperone: propeptide release modulates activation precision of pro-subtilisin. *J. Biol. Chem.* **276,** 44427–44434 CrossRef Medline
21. Patricelli, M. P., Giang, D. K., Stamp, L. M., and Burbaum, J. J. (2001) Direct visualization of serine hydrolase activities in complex proteomes using fluorescent active site-directed probes. *Proteomics* **1,** 1067–1071 CrossRef Medline
22. Hasan, N. A., Choi, S. Y., Eppinger, M., Clark, P. W., Chen, A., Alam, M., Haley, B. J., Taviani, E., Hine, E., Su, Q., Tallon, L. J., Prosper, J. B., Furth, K., Hoq, M. M., Li, H., *et al.* (2012) Genomic diversity of 2010 Haitian cholera outbreak strains. *Proc. Natl. Acad. Sci. U.S.A.* **109,** E2010–E2017 CrossRef Medline
23. Rawlings, N. D., Barrett, A. J., Thomas, P. D., Huang, X., Bateman, A., and Finn, R. D. (2018) The MEROPS database of proteolytic enzymes, their substrates and inhibitors in 2017 and a comparison with peptidases in the PANTHER database. *Nucleic Acids Res.* **46,** D624–D632 CrossRef Medline
24. Siezen, R. J., and Leunissen, J. A. (1997) Subtilases: the superfamily of subtilisin-like serine proteases. *Protein Sci.* **6,** 501–523 CrossRef Medline
25. Ellis, C. N., LaRocque, R. C., Uddin, T., Krastins, B., Mayo-Smith, L. M., Sarracino, D., Karlsson, E. K., Rahman, A., Shirin, T., Bhuiyan, T. R., Chowdhury, F., Khan, A. I., Ryan, E. T., Calderwood, S. B., Qadri, F., and Harris, J. B. (2015) Comparative proteomic analysis reveals activation of mucosal innate immune signaling pathways during cholera. *Infect. Immun.* **83,** 1089–1103 CrossRef Medline
26. Tsuji, S., Yamashita, M., Nishiyama, A., Shinohara, T., Li, Z., Myrvik, Q. N., Hoffman, D. R., Henriksen, R. A., and Shibata, Y. (2007) Differential structure and activity between human and mouse intelectin-1: human

intelectin-1 is a disulfide-linked trimer, whereas mouse homologue is a monomer. *Glycobiology* **17,** 1045–1051 CrossRef Medline
27. Li, Y., and Inouye, M. (1996) The mechanism of autoprocessing of the propeptide of prosubtilisin E: intramolecular or intermolecular event? *J. Mol. Biol.* **262,** 591–594 CrossRef Medline
28. Power, S. D., Adams, R. M., and Wells, J. A. (1986) Secretion and autoproteolytic maturation of subtilisin. *Proc. Natl. Acad. Sci. U.S.A.* **83,** 3096–3100 CrossRef Medline
29. Zhu, H., Xu, B. L., Liang, X., Yang, Y. R., Tang, X. F., and Tang, B. (2013) Molecular basis for auto- and hetero-catalytic maturation of a thermostable subtilase from thermophilic *Bacillus* sp. WF146. *J. Biol. Chem.* **288,** 34826–34838 CrossRef Medline
30. Gao, X., Wang, J., Yu, D. Q., Bian, F., Xie, B. B., Chen, X. L., Zhou, B. C., Lai, L. H., Wang, Z. X., Wu, J. W., and Zhang, Y. Z. (2010) Structural basis for the autoprocessing of zinc metalloproteases in the thermolysin family. *Proc. Natl. Acad. Sci. U.S.A.* **107,** 17569–17574 CrossRef Medline
31. Jain, S. C., Shinde, U., Li, Y., Inouye, M., and Berman, H. M. (1998) The crystal structure of an autoprocessed Ser221Cys-subtilisin E-propeptide complex at 2.0 Å resolution. *J. Mol. Biol.* **284,** 137–144 CrossRef Medline
32. Foophow, T., Tanaka, S., Koga, Y., Takano, K., and Kanaya, S. (2010) Subtilisin-like serine protease from hyperthermophilic archaeon *Thermococcus kodakaraensis* with N- and C-terminal propeptides. *Protein Eng. Des. Sel.* **23,** 347–355 CrossRef Medline
33. Altschul, S. F., Gish, W., Miller, W., Myers, E. W., and Lipman, D. J. (1990) Basic local alignment search tool. *J. Mol. Biol.* **215,** 403–410 CrossRef Medline
34. Tsuji, S., Uehori, J., Matsumoto, M., Suzuki, Y., Matsuhisa, A., Toyoshima, K., and Seya, T. (2001) Human intelectin is a novel soluble lectin that recognizes galactofuranose in carbohydrate chains of bacterial cell wall. *J. Biol. Chem.* **276,** 23456–23463 CrossRef Medline
35. Hatzios, S. K., Ringgaard, S., Davis, B. M., and Waldor, M. K. (2012) Studies of dynamic protein-protein interactions in bacteria using *Renilla* luciferase complementation are undermined by nonspecific enzyme inhibition. *PLoS One* **7,** e43175 CrossRef Medline
36. Weaver, A. I., Murphy, S. G., Umans, B. D., Tallavajhala, S., Onyekwere, I., Wittels, S., Shin, J. H., VanNieuwenhze, M., Waldor, M. K., and Dörr, T. (2018) Genetic determinants of penicillin tolerance in *Vibrio cholerae*. *Antimicrob. Agents Chemother.* **62,** e01326-18 CrossRef Medline
37. Gibson, D. G., Young, L., Chuang, R. Y., Venter, J. C., Hutchison, C. A., 3rd, Smith, H. O. (2009) Enzymatic assembly of DNA molecules up to several hundred kilobases. *Nat. Methods* **6,** 343–345 CrossRef Medline
38. Mandlik, A., Livny, J., Robins, W. P., Ritchie, J. M., Mekalanos, J. J., and Waldor, M. K. (2011) RNA-Seq-based monitoring of infection-linked changes in *Vibrio cholerae* gene expression. *Cell Host Microbe* **10,** 165–174 CrossRef Medline
39. Miller, V. L., DiRita, V. J., and Mekalanos, J. J. (1989) Identification of *toxS*, a regulatory gene whose product enhances *toxR*-mediated activation of the cholera toxin promoter. *J. Bacteriol.* **171,** 1288–1293 CrossRef Medline
40. Dörr, T., Alvarez, L., Delgado, F., Davis, B. M., Cava, F., and Waldor, M. K. (2016) A cell wall damage response mediated by a sensor kinase/response regulator pair enables β-lactam tolerance. *Proc. Natl. Acad. Sci. U.S.A.* **113,** 404–409 CrossRef Medline
41. Letunic, I., and Bork, P. (2018) 20 years of the SMART protein domain annotation resource. *Nucleic Acids Res.* **46,** D493–D496 CrossRef Medline